SCIENCE AND TECHNOLOGY

Article citation info:
LIU D, WANG S, TOMOVIC MM. Degradation modeling method for rotary lip seal based on failure mechanism analysis and stochastic process. Eksploatacja i Niezawodnosc – Maintenance and Reliability 2020; 22 (3): 381–390, http://dx.doi.org/10.17531/ein.2020.3.1.

Di LIU
Shaoping WANG
Mileta M. TOMOVIC

DEGRADATION MODELING METHOD FOR ROTARY LIP SEAL BASED ON FAILURE MECHANISM ANALYSIS AND STOCHASTIC PROCESS

METODA MODELOWANIA DEGRADACJI OBROTOWEGO USZCZELNIENIA WARGOWEGO W OPARCIU O ANALIZĘ MECHANIZMU USZKODZENIA I PROCES STOCHASTYCZNY

Rotary lip seal is widely used in aircraft and its performance affects the safety of the aircraft. Hence, it is necessary to estimate useful lifetime and reliability of the seal. Degradation of rotary lip seal is always with random effects, which cannot be considered by theoretical failure mechanism analysis. Hence, in order to consider the random effects of rotary lip seal degradation, stochastic processes are applied. Furthermore, considering the monotonic degradation of the seal, Gamma process and inverse Gaussian process are selected as the candidate processes. To combine the candidate processes, Bayesian model averaging is introduced. Based on the failure mechanism analysis and numerical simulation, the theoretical wear path is predicted and corresponding linearization method is proposed. The measured degradation data is converted and the seal wear process is transformed to a linear degradation process. The model parameters and model probabilities are evaluated by fully Bayesian inference method. The effectiveness of the proposed method is verified by comparing the predicting degradation and experimental observations. The proposed method can be used to evaluate reliability and useful lifetime of rotary lip seal. According to sensitivity analysis, an effective way to improve lifetime and reliability of the seal is to increase the wear depth threshold.

Keywords: *Rotary lip seal, Failure mechanism analysis, Stochastic process, Degradation modeling, Bayesian model averaging.*

Obrotowe uszczelnienia wargowe znajdują szerokie zastosowanie w samolotach, a ich sprawność wpływa na bezpieczeństwo statków powietrznych. Oznacza to, iż szacowanie żywotności i niezawodności tego rodzaju uszczelnień ma kluczowe znaczenie. Degradacja obrotowego uszczelnienia wargowego jest zawsze związana z efektami losowymi, których nie uwzględnia teoretyczna analiza mechanizmu uszkodzenia. Dlatego też do oceny efektów losowych degradacji obrotowego uszczelnienia wargowego wykorzystuje się procesy stochastyczne, takie jak proces Gamma czy odwrotny proces Gaussa. W przedstawionej pracy, wybrane procesy degradacji łączono za pomocą metody bayesowskiego uśredniania modeli. Na podstawie analizy mechanizmów uszkodzeń i symulacji numerycznej, konwertowano uzyskane w pomiarach dane degradacyjne, co pozwoliło na przekształcenie procesu degradacji obrotowego uszczelnienia wargowego w proces liniowy. Parametry modelu i prawdopodobieństwa oceniano za pomocą metody pełnego wnioskowania bayesowskiego na podstawie obserwacji degradacji. Skuteczność przedstawionej metody weryfikowano porównując przewidywane i obserwowane wartości degradacji. Proponowaną metodę można wykorzystywać do oceny niezawodności i żywotności obrotowego uszczelnienia wargowego. Przeprowadzona analiza czułości pokazuje, że skutecznym sposobem na poprawę żywotności i niezawodności omawianego typu uszczelnienia jest zwiększenie progu uszkodzenia w postaci maksymalnej głębokości zużycia.

Słowa kluczowe: *Obrotowe uszczelnienie wargowe, mechanizm uszkodzenia, proces stochastyczny, modelowanie degradacji, bayesowskie uśrednianie modeli.*

1. Introduction

Dynamic seals are commonly applied in aircrafts, such as hydraulic system and fuel system [20, 37]. In order to meet the requirements of modern air-craft fuel system and hydraulic system, such as high speed and high sealed pressure, dynamic seals have been paid more and more attention [9, 14, 21]. Furthermore, rotary lip seal is always used in fuel system, resulting in the failure of the rotary lip seal may lead to an incredible disaster. Hence, rotary lip seal is focused in the presented research.

A fundamental sealing mechanism of rotary lip seal with reverse pumping action is based on the profile of sealing lip and the shaft-seal interference [15]. By pumping fluid from the air-side to the liquid-side, this reverse pumping action can prevent leakage [5, 29, 30, 31]. Reverse pumping rate is one of the most important sealing performance indicators. Leak is likely to occur and the seal is likely to fail when reverse pumping rate is small enough. Furthermore, without the shaft-seal interference, the reverse pumping action will be destroyed and the seal will fail.

Several researches on analyzing degradation mechanism of the rotary lip seals have been published. Guo et al. have performed a series of experiments to analyze degradation of the seal during storage, aging in oil and using in system [6,7,8]. The authors argue that the rubber aging is the most important failure factor for the seals during storage. The roughness of sealing lip surface deceases with rubber aging, resulting in the reverse pumping action weakening. Sealing lip wear is the most important failure factor for rotary lip seal during using in system. Seal wear changes the lip profile, decreases the shaft-seal interference and weakens the reverse pumping action. A storage lifetime assessment method has been proposed in our previously published paper [10]. Hence, the useful lifetime of rotary lip seal and sealing lip wear are focused in the presented research.

Based on finite elements (FE) analysis method and Archard wear equation, several researches have been published to numerically study the seal wear process. To analyze the wear of the seal used in downhole equipment, Li et al. [35] presented a numerical analysis method for hydraulic seals. The high temperature and high pressure conditions are focus. The proposed method has been validated by comparing the simulation results with experimental observations. Based on the above numerical method, Li et al. [36] proposed a thermal-structural coupled FE analysis method. The thermal behavior is coupled with structural analysis. A mesh reconstruction strategy is used to describe the evolution of seal geometry caused by wear. The proposed method can be used to provide a suggestion for the applications considering the temperature effects. Considering the effects of lubricating characteristics on the seal wear, we have proposed a multiscale wear simulation method for rotary lip seal [11]. The proposed method has been verified by experimental observations and used to study the relationship between shaft roughness and seal wear. Based on the above method, the relationship between the shaft texture and seal wear has been numerically studied in [12]. This work provides insight into the relationship between geometric features of textured shaft and the seal wear. Based on the above wear simulation method, the theoretical degradation path of rotary lip seal can be modeled and the theoretical lifetime of the seal can also be predicted based on the simulation results [3, 4].

Based on failure mechanism analysis, the theoretical wear path and theoretical lifetime can be predicted. However, the degradation of rotary lip seal is always with random effects, which cannot be considered in theoretical failure mechanism analysis. Stochastic processes are normally introduced in degradation modeling to take into account the random effects [38]. Hence, in order to consider random effects of rotary lip seal degradation, stochastic processes are applied in the present research [13, 23].

Using stochastic process to model the degradation of rotary lip seal, the degradation process, degradation path and model parameters need to determine. The degradation process of rotary lip seal is a monotonous process. Generally, inverse Gaussian (IG) process and Gamma process are suitable to describe monotonous processes [26, 28]. Hence, IG process and Gamma process are used to model the degradation process of rotary lip seal in the presented research. Generally, under enough sample conditions, Akaike information criterion (AIC) and Bayesian information criterion (BIC) can be used to select the best degradation process among the candidate processes based on degradation dataset [16, 17]. However, due to the small sample condition of rotary lip seal, it is difficult to select the best degradation process based on AIC or BIC. Normally, Bayesian model averaging (BMA) method can be used to combine the candidate degradation processes [18, 27]. Hence, BMA method is used to combine Gamma process and IG process in the presented research.

The best degradation path among the candidate paths also can be selected by AIC and BIC under enough sample conditions. For example, in [24], the best degradation path among the candidate degradation paths, including paths with constant, monotonic, and S-shaped degradation rates, is selected based on AIC. However, similar to degradation process, under small sample conditions, it is also difficult to determine degradation path based on degradation dataset. Generally, degradation path reflects the theoretical degradation feature and can be predicted based on failure mechanism analysis [33]. Hence, in the presented research, the theoretical degradation path of rotary lip seal is predicted based on failure analysis and numerical simulation. Furthermore, the degradation process is always transformed to a linear degradation process by converting the degradation observations based on a linearization approach, which is given based on the above theoretical path [1, 34]. Generally, the model parameters and process probabilities can be evaluated by Bayesian inference method with Monte Carlo simulation method [2, 19, 25].

As discussed above, based on failure mechanism analysis and stochastic process, a degradation modeling method for rotary lip seals are proposed. Comparing to the previously published researches on degradation modeling and reliability analysis on rotary lip seal, the distinguished features of this paper are as follows: (1) Stochastic process is introduced to consider the randomness of the seal degradation. (2) Degradation path is predicted based on the failure mechanism analysis and numerical simulation. Based on the calculated theoretical path, the measured degradation data is converted and the rotary lip seal degradation process is transformed to a linear process. (3) BMA method is applied to handle process uncertainty issue, evaluate the model parameters and process probabilities.

Furthermore, the presented research is further study of the authors' previously published paper [13] and corresponding application on rotary lip seal. To meet engineering practice, in the presented research, the method to predict the degradation path and corresponding linearization method are proposed for rotary lip seal. The degradation modeling and reliability analysis method is not be limited to linear degradation process anymore compared to the previously published paper. This improvement makes the stochastic process based degradation modeling method become more practicable and available in engineering practice.

The rest of this paper is as follows: Section 2 presents the stochastic process based degradation modeling method. In Section 3, the theoretical degradation path and the linearization method are proposed based on failure mechanism analysis. In Section 4, the model parameters and process probabilities are estimated by Bayesian inference method. In Section 5, the effectiveness of the proposed method is demonstrated. In Section 6, discussion and conclusions are presented.

2. Stochastic process based degradation modeling method

2.1. Bases of stochastic process

A degradation process, which can be described as stochastic process, has the following properties:

(a) $Y(t)$ has independent increments, e.g. $Y(t_4)$ - $Y(t_3)$ and $Y(t_2)$ - $Y(t_1)$ are independent only if $t_4 > t_3 > t_2 > t_1$;
(b) The initial degradation $Y(0) \equiv 0$;
(c) The increments ΔY follow

$$\Delta Y(t) \sim f\left(\Delta\Lambda(t), \theta\right) \tag{1}$$

where $\Delta Y(t)=Y(t+\Delta t)-Y(t)$ and $\Delta\Lambda(t)=\Lambda(t+\Delta t)-\Lambda(t)$, $\Lambda(t)$ is a monotonic function, and $\boldsymbol{\theta}$ is model parameter vector.

The form of probability density function (PDF), f, is determined by the selected degradation process, Gamma process and IG process in the presented research. The form of monotonic increasing function $\Lambda(t)$ is determined by the degradation path. In the presented research, it is transformed to linear process based on linearization method and the theoretical degradation path, which is calculated by degradation mechanism analysis and numerical simulation. The model parameters and model probabilities can be evaluated based on degradation dataset, including degradation observations vector $\mathbf{Y}$ and observation time vector $\mathbf{T}$:

$$\mathbf{Y} = \left[y_1, y_2, \ldots y_n\right] \tag{2}$$

$$\mathbf{T} = \left[t_1, t_2, \ldots t_n\right] \tag{3}$$

where y_i means i-th degradation observation, t_i means i-th corresponding observation time and n is the observation size.

2.2. Linear IG process based degradation model

The degradation process of the seal is transformed to linear process. In linear IG process, the degradation Y follows IG distribution, as:

$$Y(t) \sim \mathrm{IG}\left(\mu_{\mathrm{IG}} t, \lambda_{\mathrm{IG}} t^2\right) \tag{4}$$

where μ_{IG} and λ_{IG} are the process parameters. The PDF of IG distribution, $x\sim\mathrm{IG}(a_{\mathrm{IG}},b_{\mathrm{IG}})$, is given by:

$$f_{\mathrm{IG}}\left(x|a_{\mathrm{IG}}, \mathrm{b}_{\mathrm{IG}}\right) = \sqrt{\frac{b_{\mathrm{IG}}}{2\pi x^3}} \exp\left[-\frac{b\left(x-a_{\mathrm{IG}}\right)^2}{2a_{\mathrm{IG}}{}^2 x}\right], x>0 \tag{5}$$

Hence, the corresponding PDF of the degradation y is given by:

$$f_{\mathrm{IG}}\left(y|\mu_{\mathrm{IG}} t, \lambda_{\mathrm{IG}} t^2\right) = \sqrt{\frac{\lambda_{\mathrm{IG}} t^2}{2\pi y^3}} \exp\left[-\frac{\lambda_{\mathrm{IG}}\left(y-\mu_{\mathrm{IG}} t\right)^2}{2\mu_{\mathrm{IG}}^2 y}\right] \tag{6}$$

Given the predefined failure threshold, D, the corresponding reliability function is given by:

$$R_{\mathrm{IG}}\left(t|\mu_{\mathrm{IG}} t, \lambda_{\mathrm{IG}} t^2\right) = \Phi\left[\sqrt{\frac{\lambda_{\mathrm{IG}}}{D}}\left(\frac{D}{\mu_{\mathrm{IG}}}-t\right)\right] + \exp\left(\frac{2\lambda_{\mathrm{IG}} t}{\mu_{\mathrm{IG}}}\right)\Phi\left[-\sqrt{\frac{\lambda_{\mathrm{IG}}}{D}}\left(\frac{D}{\mu_{\mathrm{IG}}}+t\right)\right] \tag{7}$$

where Φ is cumulative probability function (CDF) of standard Gaussian distribution.

The corresponding mean time to failure (MTTF) is given by [22]:

$$MTTF_{\mathrm{IG}}\left(\theta_{\mathrm{IG}}\right) = \left(\frac{D}{\mu_{\mathrm{IG}}} + \frac{\mu_{\mathrm{IG}}}{\lambda_{\mathrm{IG}}}\right)\Phi\left(\frac{\sqrt{\lambda_{\mathrm{IG}} D}}{\mu_{\mathrm{IG}}}\right) + \sqrt{\frac{D}{\lambda_{\mathrm{IG}}}}\phi\left(\frac{\sqrt{\lambda_{\mathrm{IG}} D}}{\mu_{\mathrm{IG}}}\right) - \frac{\mu_{\mathrm{IG}}}{2\lambda_{\mathrm{IG}}} \tag{8}$$

where $\phi(.)$ is PDF of standard Gaussian distribution.

2.3. Linear Gamma process based degradation model

The degradation process of the seal is transformed to linear process. In linear Gamma process, the degradation Y follows Gamma distribution, as:

$$Y(t) \sim \mathrm{Ga}\left(\mu_{\mathrm{Ga}} t, \lambda_{\mathrm{Ga}}\right) \tag{9}$$

where μ_{Ga} and λ_{Ga} are the process parameters. The PDF of Gamma distribution, $y\sim\mathrm{Ga}(a_{\mathrm{Ga}},b_{\mathrm{Ga}})$, is given by:

$$f_{\mathrm{Ga}}\left(y|a_{\mathrm{Ga}}, \mathrm{b}_{\mathrm{Ga}}\right) = \frac{1}{\Gamma\left(a_{\mathrm{Ga}}\right) b_{\mathrm{Ga}}{}^{a_{\mathrm{Ga}}}} y^{a_{\mathrm{Ga}}-1} \exp\left(-y/b_{\mathrm{Ga}}\right) \tag{10}$$

where $\Gamma(\cdot)$ is Gamma function.

Hence, the corresponding PDF of the degradation is given by:

$$f_{\mathrm{Ga}}\left(y|\mu_{\mathrm{Ga}} t, \lambda_{\mathrm{Ga}}\right) = \frac{y^{\mu_{\mathrm{Ga}} t-1}}{\Gamma\left(\mu_{\mathrm{Ga}} t\right) \lambda_{\mathrm{Ga}}{}^{\mu_{\mathrm{Ga}} t}} \exp\left(-\frac{y}{\lambda_{\mathrm{Ga}}}\right) \tag{11}$$

The corresponding reliability function is given by:

$$R_{\mathrm{Ga}}\left(t\middle|\mu_{\mathrm{Ga}} t, \lambda_{\mathrm{Ga}}\right) = 1 - \frac{\Gamma\left(\mu_{\mathrm{Ga}} t, D/\lambda_{\mathrm{Ga}}\right)}{\Gamma\left(\mu_{\mathrm{Ga}} t\right)} \tag{12}$$

The corresponding MTTF is given by [32]:

$$MTTF_{\mathrm{Ga}}\left(\theta_{\mathrm{Ga}}\right) = \frac{D}{\mu_{\mathrm{Ga}}\lambda_{\mathrm{Ga}}} + \frac{1}{2\mu_{\mathrm{Ga}}} \tag{13}$$

2.4. BMA model fusion method

Considering monotonic degradation of rotary lip seal, IG process and Gamma process are selected as candidate degradation processes. As discussed above, under enough sample conditions, the best fitting degradation process among the candidate processes can be selected by AIC and BIC. However, due to the small sample condition of rotary lip seal, it is difficult to select the best fitting degradation process among the candidate degradation processes. Hence, IG process and Gamma process are combined by BMA method. Based on Bayesian inference, the posterior model probabilities can be inferred based on Eq. (14) and used to fuse the candidate models:

$$P\left(M_i|\mathbf{Y},\mathbf{T}\right) = \frac{P\left(M_1\right) L\left(M_1|\mathbf{Y},\mathbf{T}\right)}{\sum_{i=1}^{2} P\left(M_i\right) L\left(M_i|\mathbf{Y},\mathbf{T}\right)} \tag{14}$$

where $L(M_i|\mathbf{Y},\mathbf{T})$ is likelihood of model M_i, $P(M_i|\mathbf{Y},\mathbf{T})$ is posterior probability of that the model M_i is the true model for degradation dataset, $\mathbf{Y}$ and $\mathbf{T}$, $P(M_i)$ is the prior for model probability of M_i. Furthermore, in the following parts of this paper, M_1 means M_{IG}, M_2 means M_{Ga}, and:

$$P\left(M_1\right) = \begin{cases} p_1 & M_{\mathrm{IG}} \text{ is true} \\ 0 & M_{\mathrm{Ga}} \text{ is true} \end{cases} \tag{15}$$

$$P\left(M_2\right) = \begin{cases} p_2 & M_{\mathrm{Ga}} \text{ is true} \\ 0 & M_{\mathrm{IG}} \text{ is true} \end{cases} \tag{16}$$

3. Failure mechanism analysis of rotary lip seal

As discussed above, seal wear is the most important failure factor for the seal during using in system and selected to be the degradation indictor in the presented research. Hence, the theoretical wear process is seemed as the theoretical degradation path of rotary lip seal. In this section, the wear simulation method for the seal, proposed in our previously published paper [11], is used and combined with moving-node updating strategy [4] to calculate the theoretical wear path. The maximum wear depth is selected as the degradation indicator of the seal, because it is much bigger than the minimum wear depth and the most significant wear is generally given with the most attention [11]. Furthermore, without the shaft-seal interference, the reverse pumping action will be destroyed and the seal will fail. Hence, the failure threshold of wear depth, D_w, is set as the initial shaft-seal interference.

3.1. Wear analysis of rotary lip seal

Based on our previously published wear simulation method and moving-node updating strategy, the main wear degradation simulation methodology is shown in Fig. 1, where h_w is wear depth, k_L is wear module, p_n is normal pressure, L_x is circumferential length of simulation space of microscale mixed lubrication model, L_y is axial length of that, U is translational speed of shaft and ω is rotational speed of shaft. Four steps need to perform to predict the theoretical wear path. First, evaluate lubrication characteristics and calculate wear module based on the microscale mixed thermo-elasto-hydrodynamic (TEHD) lubrication model. Second, simulate the normal pressure based on macroscale FE model of the seal. Third, calculate wear depth based on the above wear module and normal pressure. Finally, update the sealing lip profile and FE model. Repeat the above steps until the degradation time limitation is reached.

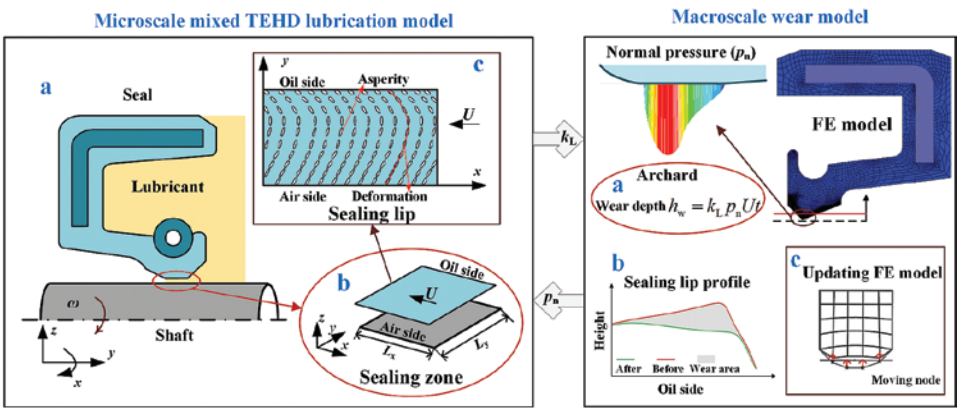

Fig. 1. Schematic diagram of wear degradation model

3.2. Theoretical degradation path and the corresponding linearization approach

Based on the above wear model and numerical simulation, the theoretical wear depth curve is predicted. By fitting the simulation results, the fitted theoretical wear path is obtained, which can be given by Eq. (17). Furthermore, the corresponding fitting results are shown in Fig. 2. It can be seen that, the theoretical wear path is not one of the common used degradation paths. Namely, even though under enough sample conditions, it is still difficult to selected the best fitting degradation path among the candidate paths based on AIC or BIC, because the theoretical wear path may not be included in the candidate paths. Hence, it is necessary to predict the wear path of rotary lip seal based on degradation mechanism analysis:

$$h_w = 54.98\ln(t+170.1) - 282.2 \tag{17}$$

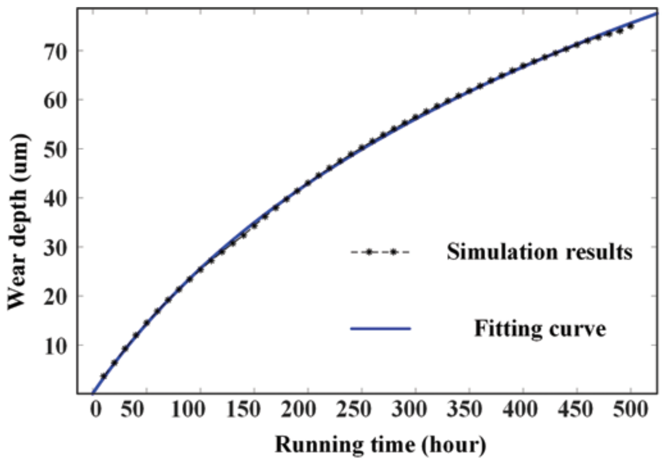

Fig. 2. Fitting results

Based on the above theoretical wear path, the linearization approach is given as follows. To transform the wear depth degradation path to a linear degradation path, the degradation of rotary lip seal is defined as:

$$y = e^{\frac{h_w + 282.2}{54.98}} - 170.1 \tag{18}$$

By transforming the degradation observations, the wear depth, based on Eq. (18), the wear depth path is transformed to a linear degradation path, as:

$$\Lambda(t) = t \tag{19}$$

Furthermore, the failure threshold, D, is also transformed from the failure threshold of wear depth, D_w, based on Eq. (18). Namely:

$$D = e^{\frac{D_w + 282.2}{54.98}} - 170.1 \tag{20}$$

4. Parameters estimation

Fully Bayesian inference is applied to estimate the model parameters and model probabilities. Considering small sample conditions of rotary lip seals and lack of prior related information, the priors are obtained based on MLE results for single candidate model.

4.1. Maximum likelihood estimation for IG process

Given the gradation dataset, $\mathbf{Y}$ and $\mathbf{T}$, the corresponding likelihood function of IG process is given by:

$$L\left(\mathbf{Y} \middle| \theta_{IG}, M_{IG}, \mathbf{T}\right) = \prod_{j=1}^{n} \sqrt{\frac{\lambda_{IG} t_j^{\,2}}{2\pi y_j^3}} \exp\left[-\frac{\lambda_{IG}\left(y_j - \mu_{IG} t_j\right)^2}{2\mu_{IG}^2 y_j}\right] \tag{21}$$

where M_{IG} means IG process and $\boldsymbol{\theta}_{IG}=(\mu_{IG},\lambda_{IG})$ is corresponding parameter vector.

The corresponding log-likelihood function is given by:

$$l\left(\boldsymbol{\theta}_{IG}|\mathbf{Y},M_{IG},\mathbf{T}\right)=\sum_{j=1}^{n}\left\{\frac{1}{2}\ln\left(\lambda_{IG}\right)+\ln\left(t_j\right)-\frac{1}{2}\ln\left(2\pi\right)-\frac{3}{2}\ln\left(y_j\right)-\frac{\lambda_{IG}\left(y_j-t_j\mu_{IG}\right)^2}{2\mu_{IG}^2 y_j}\right\} \tag{22}$$

The corresponding derivatives are given by:

$$\begin{cases}\dfrac{\partial l\left(\boldsymbol{\theta}_{IG}|\mathbf{Y},\mathbf{T},M_{IG}\right)}{\partial\lambda_{IG}}=\dfrac{A_{IG}}{\lambda_{IG}}-\dfrac{B_{IG}}{\mu_{IG}^2}+\dfrac{C_{IG}}{\mu_{IG}}-D_{IG}\\ \dfrac{\partial l\left(\boldsymbol{\theta}_{IG}|\mathbf{Y},\mathbf{T},M_{IG}\right)}{\partial\mu_{IG}}=\dfrac{B_{IG}\lambda_{IG}}{\mu_{IG}^3}-\dfrac{C_{IG}\lambda_{IG}}{\mu_{IG}^2}\end{cases} \tag{23}$$

where:

$$\begin{cases}A_{IG}=\dfrac{n}{2}\\ B_{IG}=\displaystyle\sum_{j=1}^{n}y_j\\ C_{IG}=\displaystyle\sum_{j=1}^{n}t_j\\ D_{IG}=\dfrac{1}{2}\displaystyle\sum_{j=1}^{n}\frac{t_j^2}{y_j}\end{cases} \tag{24}$$

Hence, the maximum likelihood estimation (MLE) of $\boldsymbol{\theta}_{IG}=(\mu_{IG},\lambda_{IG})$ is given by:

$$\begin{cases}\hat{\mu}_{IG}=\dfrac{B_{IG}}{C_{IG}}\\ \hat{\lambda}_{IG}=\dfrac{A_{IG}}{D_{IG}}\end{cases} \tag{25}$$

4.2. Maximum likelihood estimation for Gamma process

The likelihood function of Gamma process is given by:

$$L\left(\mathbf{Y}\middle|\boldsymbol{\theta}_{Ga},M_{Ga},\mathbf{T}\right)=\prod_{j=1}^{n}\frac{y_j^{\mu_{Ga}t_j-1}}{\Gamma\left(\mu_{Ga}t_j\right)\lambda_{Ga}^{\mu_{Ga}t_j}}\exp\left(-\frac{y_j}{\lambda_{Ga}}\right) \tag{26}$$

where θGa=(μGa,λGa) is parameter vector of Gamma process and MGa means Gamma process.

The corresponding log-likelihood function is given by:

$$l\left(\boldsymbol{\theta}_{Ga}|\mathbf{Y},M_{Ga},\mathbf{T}\right)=\sum_{j=1}^{n}\left\{\left(t_j\mu_{Ga}-1\right)\ln\left(y_j\right)-\ln\left(\Gamma\left(t_j\mu_{Ga}\right)\right)-\mu_{Ga}t_j\ln\left(\lambda_{Ga}\right)-\frac{y_j}{\lambda_{Ga}}\right\} \tag{27}$$

The corresponding derivatives are given by:

$$\begin{cases}\dfrac{\partial l\left(\boldsymbol{\theta}_{Ga}|\mathbf{Y},\mathbf{T},M_{Ga}\right)}{\partial\mu_{Ga}}=A_{Ga}-\displaystyle\sum_{j=1}^{n}t_j\psi\left(t_j\mu_{Ga}\right)-B_{Ga}\ln\left(\lambda_{Ga}\right)\\ \dfrac{\partial l\left(\boldsymbol{\theta}_{Ga}|\mathbf{Y},\mathbf{T},M_{Ga}\right)}{\partial\lambda_{Ga}}=-\dfrac{B_{Ga}\mu_{Ga}}{\lambda_{Ga}}+\dfrac{2C_{Ga}}{\lambda_{Ga}^2}\end{cases} \tag{28}$$

where $\psi\left(x\right)=\dfrac{\Gamma'\left(x\right)}{\Gamma\left(x\right)}$, $\Gamma'\left(x\right)$ means derivative function of $\Gamma\left(x\right)$ and:

$$\begin{cases}A_{Ga}=\displaystyle\sum_{j=1}^{n}t_j\ln\left(y_j\right)\\ B_{Ga}=\displaystyle\sum_{j=1}^{n}t_j\\ C_{Ga}=\displaystyle\sum_{j=1}^{n}y_j\end{cases} \tag{29}$$

Hence, the MLE of $\boldsymbol{\theta}_{Ga}=(\mu_{Ga},\lambda_{Ga})$ can be calculated based on:

$$\begin{cases}0=A_{Ga}-\displaystyle\sum_{j=1}^{n}t_j\psi\left(t_j\mu_{Ga}\right)-B_{Ga}\ln\left(\lambda_{Ga}\right)\\ 0=-\dfrac{B_{Ga}\mu_{Ga}}{\lambda_{Ga}}+\dfrac{2C_{Ga}}{\lambda_{Ga}^2}\end{cases} \tag{30}$$

4.3. Priors

Based on the above MLE results, the priors of model parameters are set by Eq. (31) and Eq. (32), respectively. For the illustrative example in the presented research, the variances are set to be one-tenth of MLE results. It should be noted that the above MLE neglects the relationship between the candidate models. Hence, the above MLE results are not the final evaluation results and can be used to set the priors of model parameters.

$$\begin{cases}\pi\left(\mu_{IG}\right)\sim\mathrm{TN}\left(\hat{\mu}_{IG},0.01\hat{\mu}_{IG}^{\,2},0,+\infty\right),\\ \pi\left(\lambda_{IG}\right)\sim\mathrm{TN}\left(\hat{\lambda}_{IG},0.01\hat{\lambda}_{IG}^{\,2},0,+\infty\right)\end{cases} \tag{31}$$

$$\begin{cases}\pi\left(\mu_{Ga}\right)\sim\mathrm{TN}\left(\hat{\mu}_{Ga},0.01\hat{\mu}_{Ga}^{\,2},0,+\infty\right)\\ \pi\left(\lambda_{Ga}\right)\sim\mathrm{TN}\left(\hat{\lambda}_{Ga},0.01\hat{\lambda}_{Ga}^{\,2},0,+\infty\right)\end{cases} \tag{32}$$

where $\hat{\mu}_{IG}$ and $\hat{\lambda}_{IG}$ are the MLE results for IG process, as shown in Eq. (25). $\hat{\mu}_{Ga}$ and $\hat{\lambda}_{Ga}$ are the MLE results for Gamma process, Eq. (30). TN(·,·,0,+∞) means truncated normal (TN) distribution and the corresponding PDF is given by:

$$f_{\mathrm{TN}}\left(x|\mu_x,\sigma_x,0,+\infty\right)=\begin{cases}\dfrac{\phi\left(\dfrac{x-\mu_x}{\sigma_x}\right)}{1-\Phi\left(\dfrac{-\mu_x}{\sigma_x}\right)} & 0\le x\\ 0 & \text{other}\end{cases} \tag{33}$$

The model prior probabilities generally can be determined based on expert experience and previous degradation data. However, the non-informative priors are always used under non prior information conditions. In the presented work, adopting non-informative prior, the priors of model probabilities are set as:

$$p_1=p_2=0.5 \tag{34}$$

4.4. Fully Bayesian inference

Fully Bayesian inference method is introduced to evaluate the model parameters and model probabilities, Eq. (35). The posterior distributions of model parameters and model probabilities can be obtained based on Eq. (36) using software OpenBUGS by Markov Chain Monte Carlo (MCMC) method. Furthermore, mean values of posterior distributions are used to evaluate the model parameters and model probabilities.

$$p\left(\boldsymbol{\theta},M|\mathbf{Y},\mathbf{T}\right)=\frac{\sum_{k=1}^{2}L\left(\mathbf{Y}\,|\boldsymbol{\theta}_k,M_k,\mathbf{T}\right)\pi\left(\boldsymbol{\theta}_k\right)\pi\left(M_k\right)}{\sum_{k=1}^{2}\int_{\boldsymbol{\theta}_k}L\left(\mathbf{Y}\,|\boldsymbol{\theta}_k,M_k,\mathbf{T}\right)\pi\left(\boldsymbol{\theta}_k\right)\pi\left(M_k\right)d\boldsymbol{\theta}_k} \tag{35}$$

$$p\left(\boldsymbol{\theta},M|\mathbf{Y},\mathbf{T}\right)\propto L\left(\mathbf{Y}|\mu_{\mathrm{IG}},\lambda_{\mathrm{IG}},\mu_{\mathrm{Ga}},\lambda_{\mathrm{Ga}},p_1,p_2\right)\pi\left(\mu_{\mathrm{IG}},\lambda_{\mathrm{IG}},\mu_{\mathrm{Ga}},\lambda_{\mathrm{Ga}},p_1,p_2\right) \tag{36}$$

where $\boldsymbol{\theta}_1$=$\boldsymbol{\theta}_{\mathrm{IG}}$, $\boldsymbol{\theta}_2$=$\boldsymbol{\theta}_{\mathrm{Ga}}$, $\boldsymbol{\theta}$=($\boldsymbol{\theta}_1$, $\boldsymbol{\theta}_2$). $\pi(\boldsymbol{\theta}_k)$ is the priors of model parameters of k-th candidate model and set based on the MLE results, as shown in Section 4.3. $\pi(M_k)$ is priori probability of k-th candidate model and non-informative prior is used, as shown in Eq. (34).

4.5. Estimation procedure

The parameters estimation procedure is shown in Fig. 3. Three steps need to perform to evaluate the model parameters and model probabilities. First, based on the degradation dataset, calculate MLE of each candidate model. Second, the priors are set based on the MLE results and non-informative prior. Finally, based on above priors and likelihood function, the posterior distributions of model probabilities and model parameters are obtained by fully Bayesian inference method. Furthermore, the model probabilities and model parameters are evaluated based on the mean values of the above posterior distributions. The algorithm for the case study in the presented research is as shown in Algorithm 1. n_{S} is beginning number of the transformed degradation observation and n_{E} is ending number transformed degradation observation. In the case study, nineteen degradation observation are measured. Furthermore, to demonstrate the effectiveness of the proposed method, the last four transformed degradation observations are retained as cross-validation observations. Hence, the beginning number n_{S}=15 and the ending number n_{E}=18.

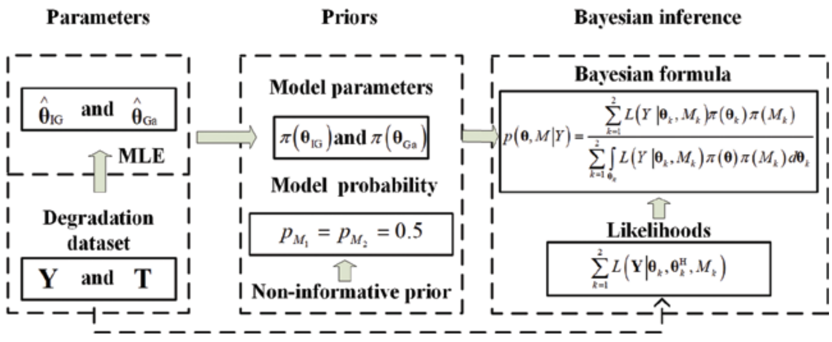

Fig. 3. Parameters estimation procedure

Algorithm 1. Simulation for case study in the presented research

Predict the theoretical wear path based on the wear analysis method, see Section 3.1.
Fit the simulation results of seal wear depth, Eq. (17)
Convert the experimental observations of wear depth based on Eq. (18).
Convert the failure threshold of wear depth to the threshold of the defined degradation based on Eq. (20).
For i=n_{S}: n_{E}
Calculate the MLE of the candidate models based on the first i transformed degradation observations, see Section 4.1 and Section 4.2.
Set the priors of the model parameters and model probabilities based on the above MLE results, see Section 4.3 and Eq. (31)-Eq (34).
Infer the model parameters and model probabilities based on the above priors and Bayesian inference, see Section 4.4.
Estimate the model parameters and model probabilities based on the mean values of the above inferring results.
Predict the degradation at the (i+1)-th predicting time.
End for
Calculate the reliability curve based on the above estimated results.
Calculate the MTTF curve based on the above estimated results.

5. Case study

In order to validate the proposed method, a typical rotary lip seal has been tested. The tested seal is as same as that presented in Ref. [12].

5.1. Experimental approach

The schematic diagram and photograph of the test bench are shown in Fig. 4. The motor is used to drive the shaft. The speed sensor is installed between the motor and shaft to measure the shaft speed. In the presented case, the shaft speed is 5000 rpm. There are two rotary lip seals are installed in the test bench. The bottom one is the tested sample. The top one is only used to seal the tank. A thermocouple is put into the sealing tank to measure oil temperature, which is controlled by adjusting the flow rates of oil in and oil out. In the presented case, the oil temperature is controlled around 25°C. Furthermore, the sealed pressure is also controlled by adjusting the flow rates of oil in and oil out. The sealed pressure is 0.2 MPa in the presented case. The sealing lip profile is measured by a profilometer. The seal wear depth is recorded every 20 hours for the first 15 observations and 50 hours for last 4 observations.

4.2. Discussions

The degradation plots of the seal wear depth by experiment are shown in Fig. 5. It can be seen that it is

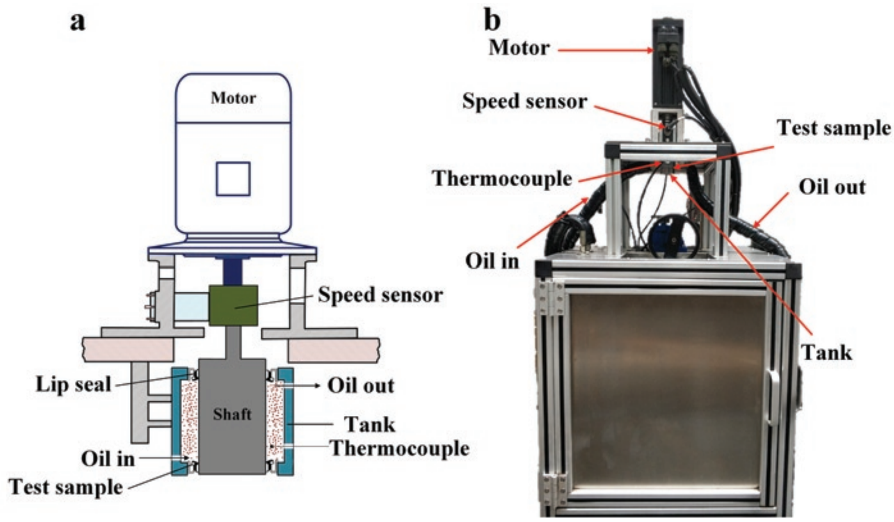

Fig. 4. (a) Schematic diagram of the test bench and (b) Photograph of the test bench

difficult to predict the degradation path of the seal wear depth. Hence, it is necessary to predict the degradation path based on the failure mechanism analysis. In the presented research, the measured seal wear depth is transformed to the defined degradation, Eq.. The transformed degradation observations are shown in Fig. 6. It can be seen that the transformed degradation observations obviously follows a linear degradation process. Namely, the theoretical wear path and the corresponding linearization method are suitable and effective. In the presented case, to validate the proposed degradation modeling method, the observations are transformed based on the above method, Eq., and are used to evaluate the model parameters and probabilities. Furthermore, to demonstrate the effectiveness of the proposed method, the last four transformed degradation observations are retained as cross-validation observations.

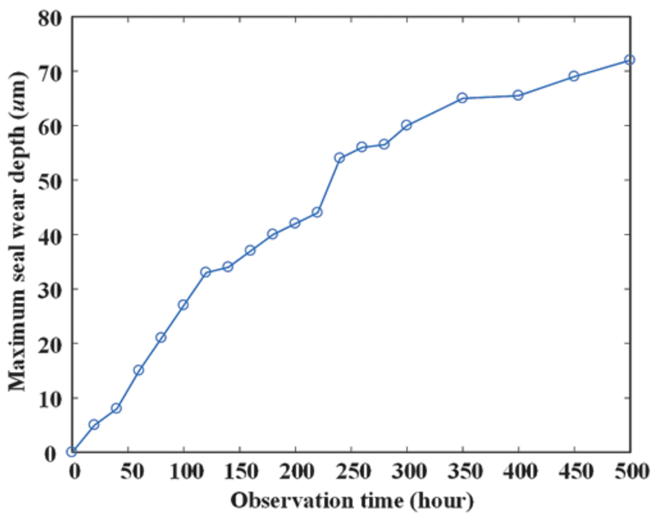

Fig. 5. Observed degradation data

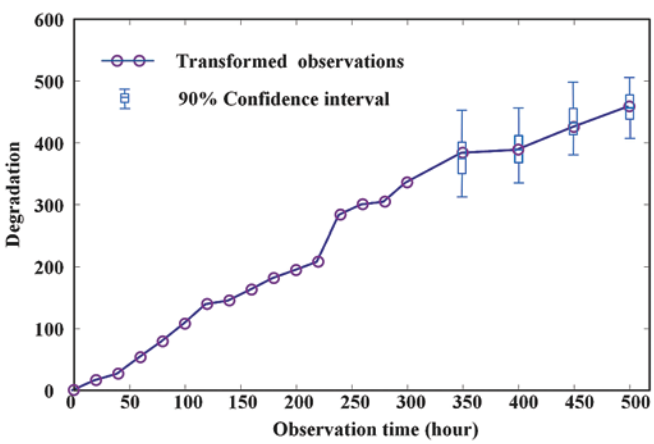

Fig. 6. Transformed degradation observation

The prediction procedure is shown in Algorithm 1. For example, to predict the degradation at 350 hours, based on the first fifteen transformed degradation observations, for each candidate model, the parameters are evaluated by MLE. The MLE results are shown in Table 1. It should be noted that the above MLE calculation neglects the relationship between the candidate models. Hence, the above MLE results are not the final estimation results and just used to set the priors of model parameters.

Table 1. MLE results based on the first fifteen degradation observations

Parameter	μ_{IG}	λ_{IG}	μ_{Ga}	λ_{Ga}
MLE results	1.0563	0.0065	0.2113	2.9212

Based on the above MLE results, according to Eq. (31) and Eq. (32), the priors for the model parameters are set as Eq. (37) and Eq. (38), respectively:

$$\begin{cases} \pi(\mu_{IG}) \sim \mathrm{TN}\left(1.0563, 0.10563^2, 0, +\infty\right), \\ \pi(\lambda_{IG}) \sim \mathrm{TN}\left(0.0065, 0.00065^2, 0, +\infty\right) \end{cases} \tag{37}$$

$$\begin{cases} \pi(\mu_{Ga}) \sim \mathrm{TN}\left(0.2113, 0.02113^2, 0, +\infty\right) \\ \pi(\lambda_{Ga}) \sim \mathrm{TN}\left(2.9212, 0.29212^2, 0, +\infty\right) \end{cases} \tag{38}$$

To predict the degradation at 350 hours. Based on the above priors of model probabilities and model parameters, the model parameters and model probabilities are estimated by fully Bayesian inference method, Eq. (36), with MCMC method using OpenBUGS [13]. The posterior model probabilities are shown in Fig. 7. It can be seen that both the Gamma process and the IG process are possibly the true degradation model for the seal. Hence, it is necessary to consider the degradation process uncertainty and combine the candidate processes. Furthermore, the MCMC simulation results for model parameters are shown in Table 2. The mean values are used to evaluate the model parameters. Based on the above evaluated model probabilities and model parameters, the degradation at 350 hours can be predicted.

Furthermore, to validate the predicting accuracy of the proposed method, the last four degradation observations are retained as cross-validation observations. The prediction procedure is as same as the above predicting procedure for predicting the degradation at 350 hours. Namely, the all observations measured before the predicting time are used to estimate the model probabilities and model parameters for predicting the degradation at the predicting time. The predicting results are shown in Fig. 8. Based on the predicting results and the last five transformed degradation observations, it can be seen that

Table 2. Model parameters' MCMC simulation results based on the first fifteen degradation observations

Parameter	Mean	Standard deviation	Upper band (2.5%)	Lower band (97.5%)
μ_{IG}	1.058	0.3233	0.4266	1.692
λ_{IG}	0.02298	0.01666	0.0009685	0.06204
μ_{Ga}	0.3745	0.0584	0.2771	0.5051
λ_{Ga}	2.889	0.4354	2.094	3.798

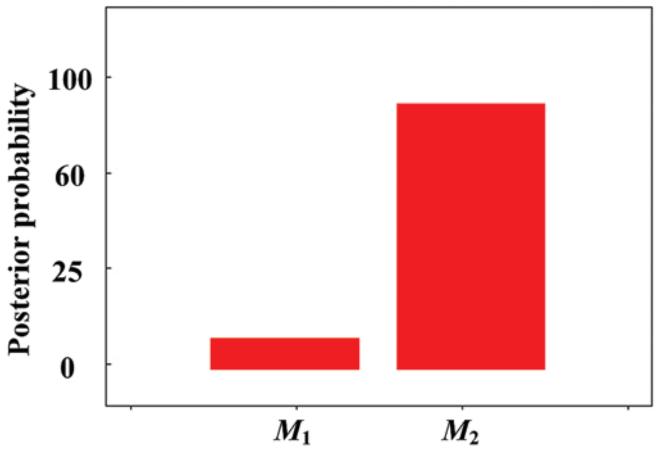

Fig. 7. Posterior probabilities of candidate models

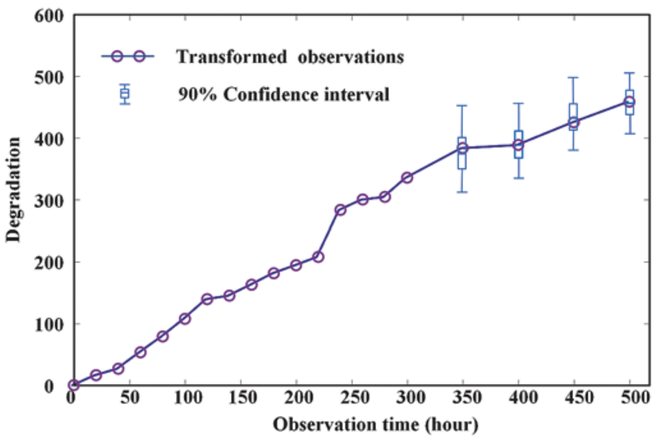

Fig. 8. Degradation prediction

the proposed method can predict the degradation of the seal precisely. Hence, the effectiveness of the proposed method has been verified.

Based on the proposed method, the reliability curve and useful lifetime distribution of the seal can also be given, Fig. 9 and Fig. 10, respectively. According to the reliability curve, the rotary lip seal can guarantee high reliability, better than 0.9, for the first 700 hours. Then the reliability of the seal quickly decreases from 700 hours to 900 hours. After 900 hours, the rotary lip seal is too unreliable to be used. According the useful lifetime distribution, it has high probability that the useful lifetime is around 800 hours. Furthermore, according to the reliability curve and useful lifetime distribution, the high reliable useful lifetime is about 750 hours for the tested rotary lip seal.

Based on the proposed method, the MTTF can also be evaluated. To investigate the sensitivity of MTTF to the failure threshold of the seal wear depth, D_w, the MTTFs under different failure thresholds are calculated and shown in Fig. 11. In the presented case, the initial seal-

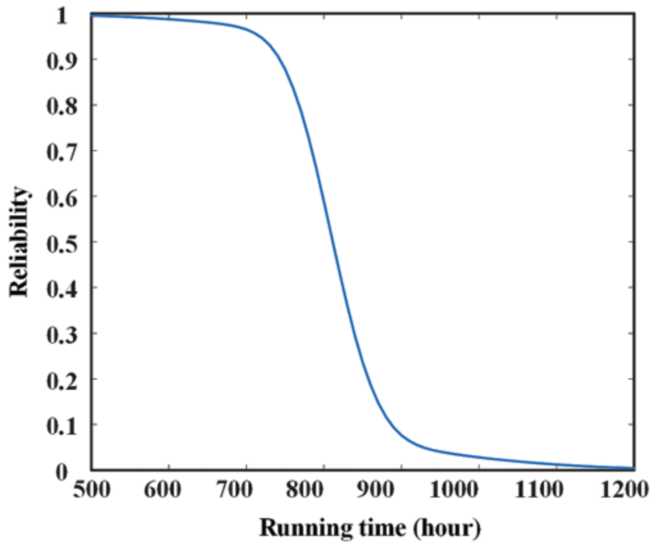

Fig. 9. Reliability curve depth

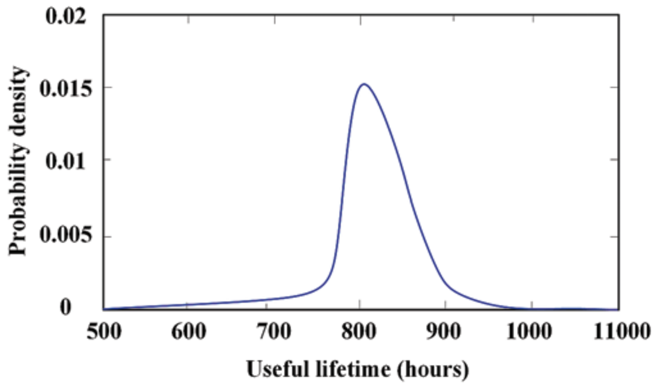

Fig. 10. Useful lifetime distribution

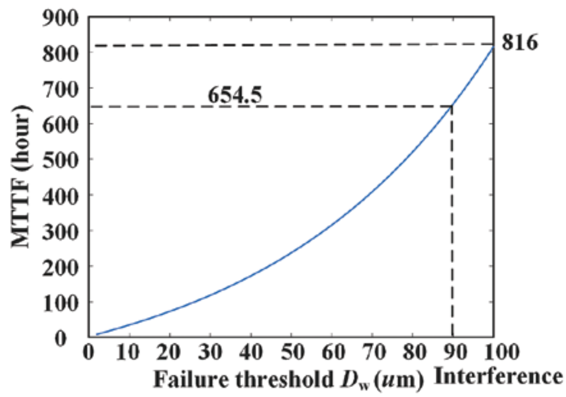

Fig. 11. Relationship between MTTF and failure threshold of maximum wear depth

shaft interference is 100um. The reverse pumping action is based on the seal-shaft interference, so the failure threshold of seal wear depth should be smaller than the initial seal-shaft interference. The MTTF is about 654.5 hours when the failure threshold is set to be 90um, while the MTTF increases to 816 hours when the failure threshold is set to be 100um. Namely, the MTTF is very sensitive to the failure threshold, especially when it approaching to the initial interference. Hence, an effective way to improve useful lifetime of the seal is to increase the failure threshold of seal wear depth, for example improving reverse pumping effects by texturing shaft surface.

6. Conclusions

In this paper, a degradation modeling method for rotary lip seal is proposed based on failure mechanism analysis and stochastic process. Stochastic process is introduced to consider randomness of rotary lip seal degradation. Considering monotonous degradation of rotary lip seal, Gamma process and IG process are selected as the candidate models and combined by BMA method. The theoretical wear path is predicted by the failure mechanism analysis and numerical simulation. A linearization method is proposed based on the theoretical wear path. In order to transform the degradation process of rotary lip seal to a linear process, the measured degradation data is transformed based on the linearization method. The model parameters and probabilities are evaluated by fully Bayesian inference method. The effectiveness of the proposed method has been verified by comparing the predicting degradation and experimental observations.

Based on the proposed method, the MTTF, reliability curve and useful lifetime distribution of the tested rotary lip seal can also be evaluated. The sensitivity of MTTF to the failure threshold of seal wear depth is analyzed. It can be seen that the MTTF is very sensitive to the failure threshold, especially when it is approaching to the initial interference. Hence, an effective way to improve useful lifetime of the seal is to increase the failure threshold of the seal wear depth, for example improving reverse pumping effect by texturing shaft surface.

The presented work provides a foundation to evaluate the useful lifetime and reliability of rotary lip seals. Future works will focus on how to improve the reverse pumping action and seal wear by texturing the shaft surface.

Acknowledgement

This study was co-supported by the National Natural Science Foundation of China (51620105010, 51575019), Natural Science Foundation of Beijing Municipality (17L10011), and Program 111.

References

1. Adrian ER, David M, Jennifer A. Bayesian Model Averaging for Linear Regression Models. Journal of the American Statistical Association 1997; 92: 179-91, https://doi.org/10.1080/01621459.1997.10473615.
2. Cao W, Jia X, Liu Y, Hu QW, Zhao JM. Selective maintenance optimisation considering random common cause failures and imperfect maintenance. Proceedings of the Institution of Mechanical Engineers, Part O: Journal of Risk and Reliability 2019; 233(3): 427-443, https://doi.org/10.1177/1748006X18799907.
3. Chen Q, Wang S, Liu D, Zhang C. Numerical analysis of wear degradation model of rotary lip seal with multifield coupling. Proceedings of IEEE 8th International Conference on Fluid Power and Mechatronics; 2019 Apr. 10-13; Wuhan, China. New York: IEEE; 2019; p. 1-6.
4. Frölich D, Magyar B, Sauer B. A comprehensive model of wear, friction and contact temperature in radial shaft seals. Wear 2014; 311(1-2): 71-80, https://doi.org/10.1016/j.wear.2013.12.030.
5. Gadari ME, Fatu A, Hajjam M. Shaft roughness effect on elasto-hydrodynamic lubrication of rotary lip seals: experimentation and numerical simulation. Tribology International 2015; 88(2015):218-27, https://doi.org/10.1016/j.triboint.2015.03.013.
6. Guo F, Jia X, Lv M, Wang L, Salant RF. The effect of aging in oil on the performance of a radial lip seal. Tribology International 2014; 78: 187-94, https://doi.org/10.1016/j.triboint.2014.05.017.
7. Guo F, Jia X, Longke W. The effect of wear on the performance of a rotary lip seal. Journal of Tribology 2014; 136(4): 041703, https://doi.org/10.1016/j.triboint.2014.05.017.
8. Guo F, Jia X, Huang L, Salant RF. The effect of aging during storage on the performance of a radial lip seal. Polymer Degradation and Stability 2013; 98(11): 2193-200, https://doi.org/10.1016/j.triboint.2014.05.017.
9. Li G, Zhang Q, Huang E, Lei Z, Wu H, Xu G. Leakage performance of floating ring seal in cold/hot state for aero-engine. Chinese Journal of Aeronautics 2019, In press, https://doi.org/10.1016/j.cja.2019.03.004.
10. Liu D, Wang S, Zhang C, Tomovic M. Bayesian model averaging based storage lifetime assessment method for rubber sealing rings. Advances in Mechanical Engineering 2019; 11(5): 1687814019853351, https://doi.org/10.1177/1687814019853351.
11. Liu D, Wang S, Zhang C. A multiscale wear simulation method for rotary lip seal under mixed lubricating conditions. Tribology International 2018; 121: 190-203, https://doi.org/10.1016/j.triboint.2018.01.007.
12. Liu D, Wang S, Tomovic M, Zhang C. Numerical study of the effects of textured shaft on the wear of rotary lip seals. Tribology International 2019; 138: 215-38, https://doi.org/10.1016/j.triboint.2019.05.037.
13. Liu D, Wang S, Zhang C, Tomovic M. Bayesian model averaging based reliability analysis method for monotonic degradation dataset based on inverse Gaussian process and Gamma process. Reliability Engineering & System Safety 2018; 180: 25-38, https://doi.org/10.1016/j.ress.2018.06.019.
14. Liu W, He G. Storage life of silicone rubber sealing ring used in solid rocket motor. Chinese Journal of Aeronautics 2014; 27(6): 1469-76, https://doi.org/10.1016/j.cja.2014.10.013.
15. Müller HK. Concepts of sealing mechanism of rubber lip type rotary shaft seals. In: Proceedings of the BHRA 11th international conference on fluid sealing. Cannes. 1987: 698-709.
16. Park C, Padgett WJ. Stochastic degradation models with several accelerating variables. IEEE Trans Rel 2006; 55 :379-90, https://doi.org/10.1109/TR.2006.874937.
17. Park C, Padgett WJ. Accelerated degradation models for failure based on geometric Brownian motion and Gamma processes. Lifetime Data Anal 2005; 11: 511-27, https://ieeexplore.ieee.org/document/1638421.
18. Park I, Grandhi RV. A Bayesian statistical method for quantifying model form uncertainty and two model combination methods. Rel Eng Syst Safety 2014; 129: 46-56, https://doi.org/10.1016/j.ress.2014.04.023.
19. Peter JH, Malik A S, Langer K. An efficient reliability-based simulation method for optimum laser peening treatment. Journal of Manufacturing Science and Engineering 2016; 138(11): 111001, https://doi.org/10.1115/1.4033604.
20. Peng C, Guo S, Ouyang X, Zhou Q, Yang H. An eccentric 3-D fluid-structure interaction model for investigating the effects of rod parallel offset on reciprocating-seal performance. Tribology International 2018; 128: 279-90, https://doi.org/10.1016/j.triboint.2018.07.028.

21. Peng C, Ouyang X, Zhu Y, Guo S, Zhou Q, Yang H. Investigation into the influence of stretching on reciprocating rod seals based on a novel 3-D model vs axisymmetric model. Tribology International 2018; 117: 1-14, https://doi.org/10.1016/j.triboint.2017.06.020.
22. Peng CY. Inverse Gaussian processes with random effects and explanatory variables for degradation data. Technometrics 2015; 57: 100-11.
23. Peng W, Liu Y, Zhang X, Huang HZ. Sequential preventive maintenance policies with consideration of random adjustment-reduction features. Eksploatacja i Niezawodnosc -Maintenance and Reliability 2015, 17(2): 306-313, https://doi.org/10.1080/00401706.2013.879077.
24. Peng W, Li YF, Yang YJ, Mi J, Huang HZ. Bayesian Degradation Analysis With Inverse Gaussian Process Models Under Time-Varying Degradation Rates. IEEE Transactions on Reliability 2017; 66: 84-96, https://ieeexplore.ieee.org/document/7803533/.
25. Peng W, Li YF, Yang YJ, Huang HZ, Zuo MJ. Inverse Gaussian process models for degradation analysis: a Bayesian perspective. Reliab Eng Syst Saf 2014; 130: 175-89, https://doi.org/10.1016/j.ress.2014.06.005.
26. Qin H, Zhang S, Zhou W. Inverse Gaussian process-based corrosion growth modeling and its application in the reliability analysis for energy pipelines. Front. Struct. Civil Eng 2013; 7: 276-87.
27. Raftery AE, Gneiting T, Balabdaoui F, Polakowski M. Using Bayesian model averaging to calibrate forecast ensembles. Month Weather Rev 2005; 133: 1155-74.
28. Rodríguezpicón LA, Rodríguezpicón AP, Méndezgonzález LC, Rodríguez-Borbón MI, Alvarado-Iniesta A. Degradation modeling based on gamma process models with random effects. Commun Stat 2017; 1: 1-15.
29. Salant RF, Flaherty AL. Elastohydrodynamic analysis of reverse pumping in rotary lip seals with microasperities. Journal of Tribology 1995; 117(1): 53-9.
30. Shen D, Salant RF. Elastohydrodynamic analysis of the effect of shaft surface finish on rotary lip seal behavior. Tribology Transactions 2003; 46(3): 391-6.
31. Shen D, Salant RF. A transient mixed lubrication model of a rotary lip seal with a rough shaft. Tribology Transactions 2006; 49(4): 621-34.
32. Tseng ST, Balakrishnan N, Tsai CC. Optimal step-stress accelerated degradation test plan for gamma degradation processes. IEEE Transactions on Reliability 2009; 58: 611-18.
33. Wang HK, Li YF, Liu Y, Yang YJ, Huang HZ. Remaining useful life estimation under degradation and shock damage. Proceedings of the Institution of Mechanical Engineers, Part O: Journal of Risk and Reliability 2015; 229(3): 200-208.
34. Wang LZ, Pan R, Li XY, Jiang TM. A Bayesian reliability evaluation method with integrated accelerated degradation testing and field information. Reliability Engineering & System Safety 2013; 112: 38-47.
35. Li X, Peng GL, Wang Q. A numerical analysis method of hydraulic seals for downhole equipments. Advances in Mechanical Engineering 2013; 5: 151794.
36. Li X, Peng GL, Li Z. Prediction of seal wear with thermal-structural coupled finite element method. Finite Elements in Analysis and Design 2014; 83: 10-21.
37. Yang Y J, Huang HZ, Liu Y, Zhu SP, Peng WW. Reliability analysis of electrohydraulic servo valve suffering common cause failures. Eksploatacja i Niezawodnosc -Maintenance and Reliability 2014, 16(3): 354-359.
38. Zio E. Some challenges and opportunities in reliability engineering. IEEE Transactions on Reliability 2016; 65(4): 1769-82.

Di LIU
Shaoping WANG
School of Automation Science and Electrical Engineering
Beihang University
Xueyuan Road, Haidian District, Beijing, P.R. China

Mileta M. TOMOVIC
Department of Engineering Technology
Old Dominion University
Norfolk, Virginia, 23529, USA

Emails: liudi54834@buaa.edu.cn, shaopingwang@buaa.edu.cn, MTomovic@odu.edu